

Image Restoration by Lifting-Based Wavelet Domain E-Median Filter

Sema Koç and Ergun Erçelebi

In this paper, we propose a method of applying a lifting-based wavelet domain e-median filter (LBWDEMF) for image restoration. LBWDEMF helps in reducing the number of computations. An e-median filter is a type of modified median filter that processes each pixel of the output of a standard median filter in a binary manner, keeping the output of the median filter unchanged or replacing it with the original pixel value. Binary decision-making is controlled by comparing the absolute difference of the median filter output and the original image to a preset threshold. In addition, the advantage of LBWDEMF is that probabilities of encountering root images are spread over sub-band images, and therefore the e-median filter is unlikely to encounter root images at an early stage of iterations and generates a better result as iteration increases. The proposed method transforms an image into the wavelet domain using lifting-based wavelet filters, then applies an e-median filter in the wavelet domain, transforms the result into the spatial domain, and finally goes through one spatial domain e-median filter to produce the final restored image. Moreover, in order to validate the effectiveness of the proposed method we compare the result obtained using the proposed method to those using a spatial domain median filter (SDMF), spatial domain e-median filter (SDEMF), and wavelet thresholding method. Experimental results show that the proposed method is superior to SDMF, SDEMF, and wavelet thresholding in terms of image restoration.

Keywords: Lifting-based wavelet transform, image restoration, e-median filtering, classical wavelet transform.

Manuscript received Feb. 28, 2005; revised Sept. 12, 2005.

Sema Koç (phone: + 90 342 3601200, email: skoc@gantep.edu.tr) and Ergun Erçelebi (email: ercelebi@gantep.edu.tr) are with the Department of Electrical and Electronics Engineering, University of Gaziantep, Turkey.

I. Introduction

Images are often degraded by noise due to channel transmission errors (for example, binary symmetric channel noise), a faulty image acquisition device, engine sparks, ac power interference, and atmospheric electrical emissions. Due to the strong amplitude of noise, human visual perception is very sensitive to it, and the removal of such noise is an important issue in image processing. A fundamental problem in image processing is to remove the additive Gaussian noise without blurring the fine-details of the images.

A vast literature has emerged recently on image restoration using linear techniques and nonlinear techniques. Most of the linear techniques, such as averaging low-pass filters have low-pass characteristics, and they tend to blur edges and destroy lines, edges, and other fine image details. The two often-used nonlinear techniques are the median filter and the wavelet thresholding or shrinkage of Donoho and Johnstone [1]-[3]. Wavelet thresholding, which is nonlinear, is a noise reduction method by transforming a noisy image into the wavelet domain, applying thresholding in the wavelet domain, and inverse transforming the restored wavelet coefficients. Alternative approaches to nonlinear wavelet-based restoration can be found in [4] and [5]. The choice of thresholding functions and threshold values are critical in restoration schemes. Donoho [1] proposes an expression for computation of the threshold value, which is known as a universal threshold. This threshold value depends on the number of data samples. If the number of data samples is too small, the result will still be noisy. On the other hand, if it is too large, important details of the images will be removed. Due to this reason the wavelet thresholding has a drawback [6]. The other method for image restoration and noise removal, introduced by Rudin and Osher [7], was total variation (TV). TV is an integration of the length of all the gradients in any

point in a continuous signal domain. As the gradient in a point is a measure of the variation of the function in this point, integration over the entire domain must result in the total variation. Roughly speaking, the idea of minimizing the total variation is to use the L^1 norm of the gradient instead of its L^2 norm. The main problem in minimizing the TV norm comes from the non-differentiable gradient argument.

The standard median filter consists of applying a sliding window over a specified finite length sequence and replacing the center pixel in the window by the standard median of the pixels within the window [9], [10]. One problem of the standard median filter is that it tends to alter pixels undisturbed by noise [11]. Recently, different modifications of the median filter have been proposed to overcome its pitfalls. The E-median filter is a type of modified standard median filter.

In this paper, we propose an image restoration method for images corrupted by additive white Gaussian noise (AWGN). The method is based on using an iterative e-median filter in the wavelet domain. Using the median filter to eliminate additive Gaussian noise is less effective in the spatial domain, but this is not true in the wavelet domain when you consider the statistics of wavelet coefficients of natural images, so a better estimation of the variance field incorporating local characteristics of wavelet coefficients may be done by using an iterative median filter. In this study, wavelet transforms are constructed by a lifting scheme. A lifting scheme is a new method for constructing wavelets. The basic idea behind a lifting scheme is very simple. It starts with trivial wavelets, which do nothing but hold the formal properties of a wavelet. The lifting scheme then gradually constructs a new wavelet with improved properties. Classical wavelets, which are so-called first-generation wavelets, are known as translation and dilation of one fixed function; the Fourier transform is then a very important tool for first-generation wavelets. On the other hand, a construction with a lifting scheme is entirely spatial and therefore ideally suited for building second-generation wavelets when no Fourier transform is available. The lifting scheme allows a faster implementation of the wavelet transform (WT), and reducing computational time in real applications is very crucial. Moreover, no extra memory is needed and the original signal can be replaced with its WT.

In the implementation of the proposed algorithm, first the noisy image is transformed into the wavelet domain by lifting-based wavelet filters. Second, in the wavelet domain, an e-median filter is applied only to detail coefficients. Third, the sub-band images are inversely transformed to the spatial domain and go through one spatial domain e-median filter to produce the final restored image. The experimental results have shown that the performance of our proposed image restoration method is noticeably superior to that of a spatial domain median filter (SDMF), spatial domain e-median filter

(SDEMF), and wavelet thresholding. The rest of this paper is organized as follows. In section II, we review the spatial domain e-median filters. Section III introduces briefly the construction of a second-generation WT. In section IV, the lifting-based wavelet transform e-median filter is discussed. In section V, results and a relevant discussion are given. In section VI, conclusions are given.

II. Spatial Domain E-Median Filter

A standard median filter is based on moving a window of odd length over an image (as in a convolution), ranking of the pixels in a neighborhood according to brightness within the input window, and replacing the center pixel in the window by the median of the pixels within the window [10], [12]. The standard median filter is able to remove a large amount of noise, but at the same time it makes some false alarms. Because of the disadvantage of the standard median filter, modifications of the median filter have been proposed to improve the performance of the filter. One type of modified median filter is the so-called e-median filter, which has the following form [13]:

$$Z(m, n; \xi) = \begin{cases} Y(m, n) + \beta(X(m, n) - Y(m, n), \xi), \\ 0 \end{cases}$$

where $m = 1, \dots, M$, $n = 1, \dots, N$, and

$$\beta(x, \xi) = \begin{cases} x & \text{if } |x| > \xi A, \\ 0 & \text{otherwise,} \end{cases} \quad (1)$$

where X is the noisy observation image, Z refers to the restored image by the e-median filter, Y refers to the restored image by the standard median filter, ξ is a preset threshold between 0 and 1, and A is the maximum possible value of X , usually 255 in the spatial domain but it can be greater than 255 in the wavelet domain. A is obtained by computing the maximum value of each of the detail sub-bands in the wavelet domain. To quantitatively assess the performance of the e-median filter, we compute the logarithm of the mean squares error (LMSE) of the restored image. Assume we know the original image $\hat{f}(m, n)$, we can calculate the MSE of restored image Z at different ξ 's:

$$LMSE(\xi) = \log_{10} \left(\frac{1}{MN} \sum_{m=1}^M \sum_{n=1}^N (Z(m, n; \xi) - \hat{f}(m, n))^2 \right), \quad (2)$$

where $m = 1, \dots, M$, $n = 1, \dots, N$. To restore the image, it is optional to choose the ξ corresponding to the smallest LMSE. In reality, the original image is unknown, and it is impossible to

calculate the LMSE and use it as a criterion to choose ζ . Instead, we choose to use the logarithm of the Laplacian (LNL) norm of the restored image as an approximation of the LMSE and search out a ζ that minimizes the norm. We denote κ as the LNL of image Z :

$$\kappa(Z) = \log \left\| \nabla^2 Z \right\|, \quad (3)$$

where ∇^2 represents the Laplacian operation, and κ is used as a criterion to select the proper ζ and is computed using the restored image only.

In image restoration, the SDEMF filter can be used iteratively. By iteratively applying SDEMF, a root image, an image that is invariant to further median filtering, appears at an early stage of iteration, and the restoration process becomes worse [14].

As seen in Fig.1 we chose a ζ that minimizes LNL as a threshold.

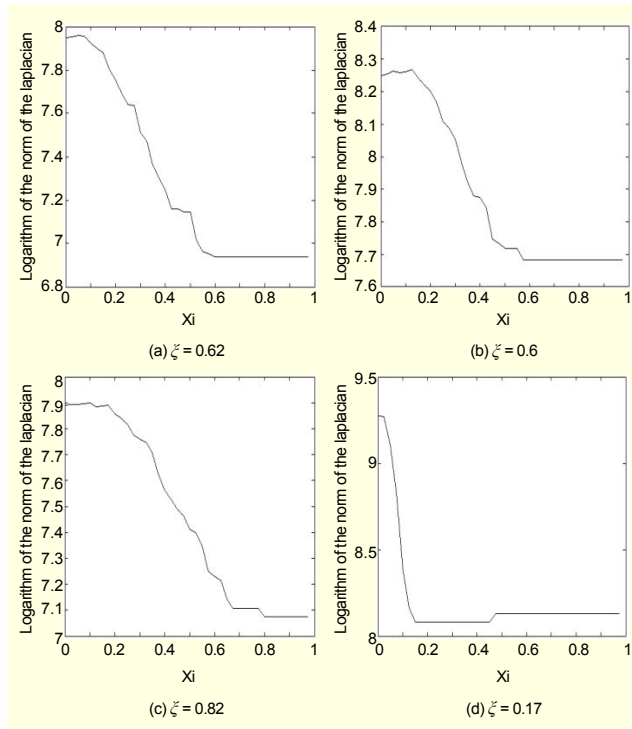


Fig. 1. (a) LNL of Z versus threshold ξ for detail high-low (HL) sub-band, (b) LNL of Z versus threshold ξ for detail low-high (LH) sub-band, (c) LNL of Z versus threshold ξ for detail high-high (HH) sub-band, and (d) LNL of Z versus threshold ξ for final image in spatial domain.

III. Lifting-Based Wavelet Transform

1. Lifting Scheme

The past 15 years have shown a steadily growing interest in

wavelet transforms and perfect reconstruction filter banks (PRFBs) as well as their application in numerous areas in signal and image processing. Various techniques to construct wavelet bases for different cases have been presented. One of these is the lifting scheme, which was first introduced by Sweldens in the mid 1990's [15]-[17]. Lifting-based wavelet transform implementation helps in reducing the number of computations [18]. The conventional convolution-based implementation of the discrete wavelet transform has high computational and memory requirements. Recently, the lifting-based implementation of the discrete wavelet transform has been proposed to overcome these drawbacks [6], [16], [17], and [19]-[21].

The basic principle of the lifting scheme [19] is to factorize the polyphase matrix of a wavelet filter into a sequence of alternating upper and lower triangular matrices and a diagonal matrix with constants. The factorization is obtained by using an extension of the Euclidean algorithm. The resulting formulation can be implemented by means of banded matrix multiplications. Let $\tilde{h}(z)$ and $\tilde{g}(z)$ be the low- and high-pass analysis filters, and $h(z)$ and $g(z)$ be the low- and high-pass synthesis filters. The filters can be divided into even and odd parts as

$$\begin{aligned} \tilde{h}(z) &= \tilde{h}_e(z^2) + z^{-1}\tilde{h}_o(z^2), h(z) = h_e(z^2) + z^{-1}h_o(z^2), \\ \tilde{g}(z) &= \tilde{g}_e(z^2) + z^{-1}\tilde{g}_o(z^2), \text{ and } g(z) = g_e(z^2) + z^{-1}g_o(z^2). \end{aligned} \quad (4)$$

The polyphase matrices are then defined as

$$\tilde{P}(z) = \begin{bmatrix} \tilde{h}_e(z) & \tilde{h}_o(z) \\ \tilde{g}_e(z) & \tilde{g}_o(z) \end{bmatrix} \text{ and} \quad (5)$$

$$P(z) = \begin{bmatrix} h_e(z) & h_o(z) \\ g_e(z) & g_o(z) \end{bmatrix}. \quad (6)$$

It has been shown in [19] that if (\tilde{h}, \tilde{g}) is a complementary filter pair, then $\tilde{P}(z)$ can always be factored into the following lifting steps (K_1 and K_2 are constants):

$$\tilde{P}_1(z) = \begin{bmatrix} K_1 & \\ & K_2 \end{bmatrix} \prod_{i=1}^p \begin{bmatrix} 1 & \tilde{s}_i(z) \\ 0 & 1 \end{bmatrix} \begin{bmatrix} 1 & 0 \\ \tilde{t}_i(z) & 1 \end{bmatrix}, \text{ or} \quad (7)$$

$$\tilde{P}_2(z) = \begin{bmatrix} K_1 & \\ & K_2 \end{bmatrix} \prod_{i=1}^p \begin{bmatrix} 1 & 0 \\ \tilde{t}_i(z) & 1 \end{bmatrix} \begin{bmatrix} 1 & \tilde{s}_i(z) \\ 0 & 1 \end{bmatrix}. \quad (8)$$

Scheme 1 corresponds to the $\tilde{P}_1(z)$ factorization and is shown in Fig. 2. Here the low-pass samples (even terms) are multiplied by the time domain equivalent of $\tilde{t}(z)$, and are added to the high-pass samples (odd terms) in the first step. In the second step, the updated high-pass samples are multiplied

by the time domain equivalent of $\tilde{s}(z)$ and are added to the low-pass samples. In scheme 2, which corresponds to the $\tilde{P}_2(z)$ factorization, the low-pass terms are calculated in the first step ($\tilde{s}(z)$ is used), and the high-pass terms are calculated in the second step ($\tilde{t}(z)$ is used). In both schemes, if a diagonal matrix is present in the factorization, the low-pass coefficients are multiplied with K_1 and the high-pass coefficients are multiplied with K_2 .

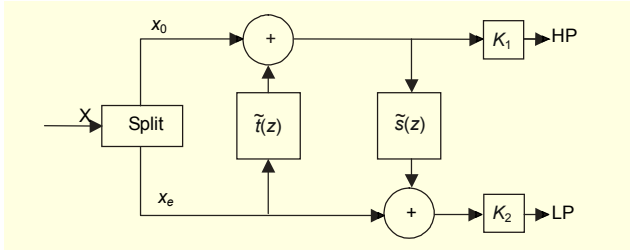


Fig. 2. Forward wavelet transform using lifting scheme.

2. Wavelet Decomposition

Let f_{xy} denote an image. Applying the lifting wavelet filters \tilde{h} and \tilde{g} to the image f_{xy} in the x -direction we can obtain low- and high-frequency components in the x -direction. After down sampling by 2, images are reduced to half on the x -direction. Equation (9) yields low- and high-frequency components of the image in the x -direction, respectively:

$$f_L(x, y) = \sum_{k=0}^{M-1} \sum_{l=0}^{N-1} f(k, l) \tilde{h}(x-k, y-l) \quad \text{and}$$

$$f_H(x, y) = \sum_{k=0}^{M-1} \sum_{l=0}^{N-1} f(k, l) \tilde{g}(x-k, y-l), \quad (9)$$

where \tilde{h} and \tilde{g} indicate low-pass and high-pass decomposition filters. In the same way as above, applying the lifting wavelet filters \tilde{h} and \tilde{g} to the two sub-images (f_L, f_H) in the y -direction, we obtain four sub-images ($f_{LL}, f_{LH}, f_{HL}, f_{HH}$). Equation (10) gives a decomposition of the image into four sub-images:

$$f_{LL}(x, y) = \sum f_L(2x, 2y) \tilde{h}_y, \quad f_{LH}(x, y) = \sum f_L(2x, 2y) \tilde{g}_y,$$

$$f_{HL}(x, y) = \sum f_H(2x, 2y) \tilde{h}_y, \quad \text{and} \quad f_{HH}(x, y) = \sum f_H(2x, 2y) \tilde{g}_y. \quad (10)$$

As seen in Fig. 3(a), a two-dimensional lifting-based wavelet transform produces one set of approximation coefficients (f_{LL}) and three sets of detail coefficients (f_{LH}, f_{HL}, f_{HH}). Further decomposition can be achieved by acting upon the f_{LL} sub-band successively, and the resultant image is split into multiple bands in Fig. 3(b). Figures 4(a) and 4(b) show decomposition of a

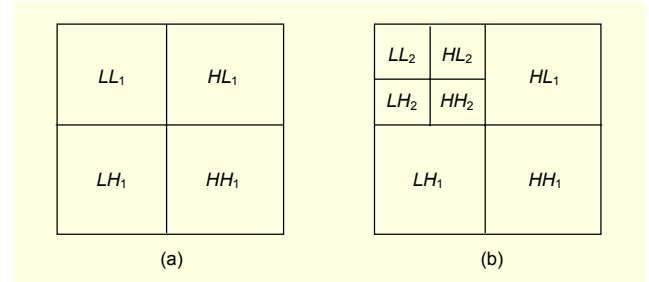


Fig. 3. Two-dimensional wavelet transform: (a) first-level decomposition and (b) second-level decomposition. (L denotes a low band, H denotes a high band, and the subscript denotes the number of the level).

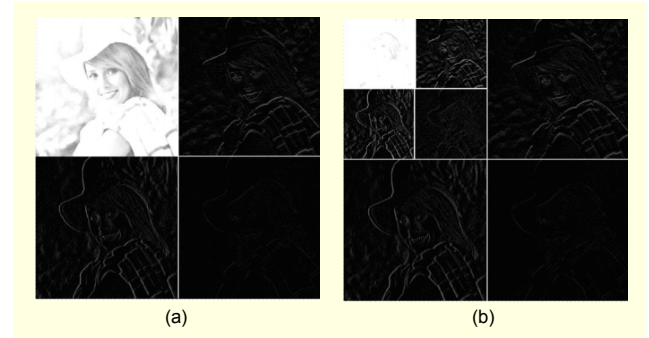


Fig. 4. (a) Original image of size 512x512, 1 level decomposition, and (b) original image of size 512x512, 2-level decomposition.

512x512 grayscale image, *Elaine*, at the first and second levels, respectively.

The reconstruction of the image can be carried out by the following procedure. First, all four sub-bands at the coarsest scale are up-sampled by a factor of 2, and the sub-bands are filtered using low-pass h and high-pass g synthesis filters in each dimension. Then, the four filtered sub-bands are merged to reach the low sub-band at the next finer scale. The process is repeated until the image is fully reconstructed.

IV. Lifting-Based Wavelet Transform E-Median Filter

A general block diagram of the proposed image restoration method is shown in Fig. 5.

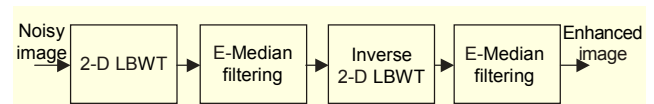


Fig. 5. Block diagram of the proposed image restoration method.

The proposed method for the image restoration is implemented as follows:

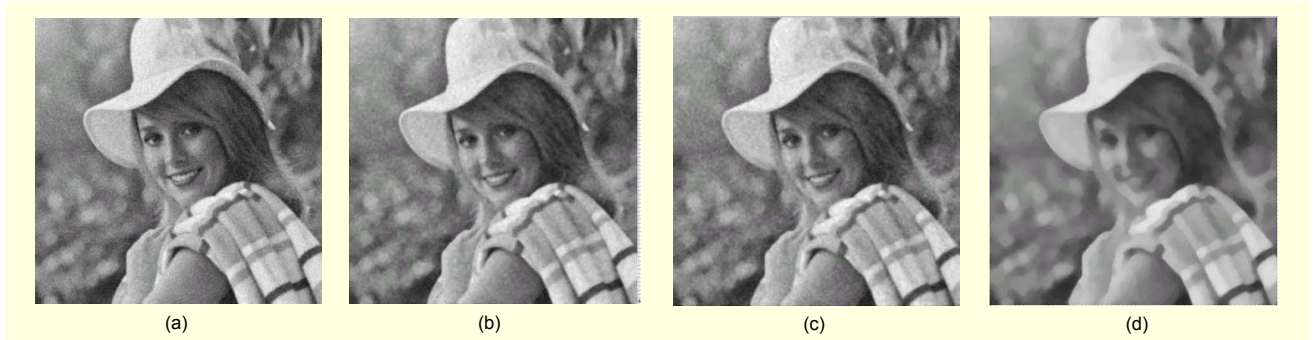


Fig. 6. (a) Corrupted image of size 512×512 (PSNR=20.19) and (b) restored image using the proposed method with DB4 filter (PSNR=31.77), (c) restored image using spatial domain e-median filter method (PSNR=29.92), and (d) restored image using spatial domain median filter method (PSNR=28.50), each after 30 iterations.

- Step 1. The noisy image is decomposed into the sub-band images, LL, LH, HL, HH , using lifting-based wavelet filters.
- Step 2. An e-median filter is carried out over three sets of detail coefficients, LH, HL, HH .
- Step 3. The peak signal-to-noise ratio (PSNR) is computed.
- Step 4. The newly computed PSNR is compared with the previous PSNR; if the newly computed PSNR is greater or equal to the previous PSNR, then the restoration process continues and the program goes to step 2. But if not, go to step 5.
- Step 5. The sub-band images are inversely transformed to the spatial domain using an inverse lifting-based Daubechies 2 (DB2), Daubechies 4 (DB4), or Haar wavelet filter and sent through one SDEMf to produce the final restored image.

V. Experimental Results

Simulations have been performed on various types of gray scale images 512×512 in size, *Elaine, Scene, and Lena*, using a mask size of 5×5 . In many cases, a relatively small window (3×3) provides satisfactory results. However, for a highly corrupted image (about 20 percent), a 2-D median filter with a small window does not suppress noise effectively. It is therefore necessary to use a relatively larger window (5×5). To evaluate the performance of the proposed method, we compared it with SDMF, SDEMf, and the wavelet thresholding method. The lifting-based wavelets in this study belong to the following families: Haar, DB2, and DB4. The performance of the method was evaluated using the PSNR. Let \hat{f} and Z denote the original and restored images, respectively. The root mean square error is given by

$$\varepsilon = \sqrt{\frac{1}{NM} \sum_k (\hat{f}_k - Z_k)^2}, \quad (11)$$

where N and M indicate the size of image. The PSNR in decibels is given by

$$PSNR = 20 \log_{10} \left(\frac{256}{\varepsilon} \right). \quad (12)$$

The corrupted image by Gaussian noise at PSNR= 20.19 is shown in Fig. 6(a). Figure 6(b) illustrates the result of the proposed method using the DB4 filter with decomposition level 1 at PSNR=31.77, while Fig. 6(c) shows the result of SDEMf at PSNR=29.92 and Fig. 6(d) shows that of SDMF at PSNR= 28.50 after 30 iterations.

Figure 7 plots the PSNR versus number of iterations for the proposed method, SDMF, and SDEMf. In Fig. 7, the 512×512 image *Lena* was used. It can be seen from Fig. 7 that the proposed method provides superior results to SDMF and SDEMf in the removal of Gaussian noise at different numbers of iteration. When the number of iterations increases, the proposed method enhances the image quality, while SDMF

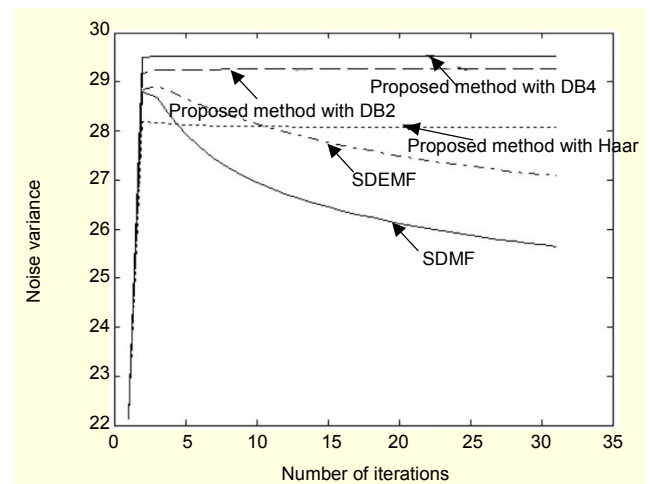


Fig. 7. PSNR versus number of iterations for the proposed method, SDMF, and SDEMf (512×512 *Lena*).

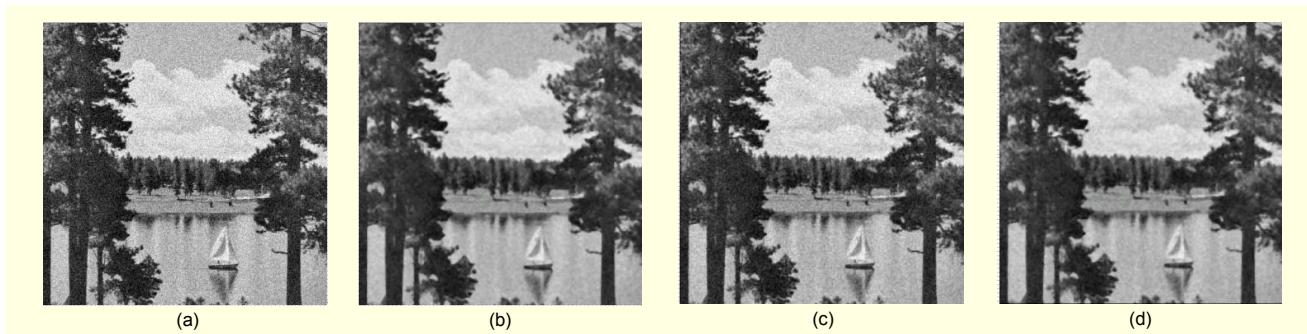


Fig. 8. (a) Corrupted image (PSNR=20.19), (b) the result of the proposed method with DB4 (PSNR=25.96), (c) the result of SDMF (PSNR=25.49), and (d) the result of SDEMf (PSNR=25.75).

Table 1. PSNR for different lifting-based wavelet filters, SDMF, SDEMf, and wavelet thresholding.

	Noisy image	Proposed algorithm			SDMF	SDEMf	Visuhard thresholding	Visusoft thresholding
		Haar	DB2	DB4				
Elaine 512×512								
$\sigma=10$	28.17	32.62	36.03	36.47	34.77	36.01	34.46	32.94
$\sigma=15$	24.65	31.23	33.95	34.70	31.77	33.93	32.88	31.72
$\sigma=20$	22.13	29.69	32.69	33.11	29.50	32.03	31.82	30.92
$\sigma=25$	20.21	28.32	31.04	31.77	27.67	30.63	30.95	30.32
$\sigma=30$	18.63	27.08	30.01	30.56	26.15	29.21	30.32	29.83
Lena 512×512								
$\sigma=10$	28.17	28.84	31.29	32.09	30.37	31.14	30.93	29.02
$\sigma=15$	24.65	28.80	30.03	30.51	29.61	29.84	29.24	27.73
$\sigma=20$	22.13	28.19	29.17	29.52	28.79	28.85	28.09	26.93
$\sigma=25$	20.21	27.73	28.61	28.80	27.95	27.97	27.35	26.36
$\sigma=30$	18.63	27.0	28.07	28.09	27.15	27.30	26.70	25.94

and SDEMf degrade it.

Figure 8(a) shows a corrupted image at PSNR=20.19, while Figs. 8(b), 8(c), and 8(d) plot the result of the proposed method, SDMF, and SDEMf, respectively. It is obvious from Fig. 8 that our method shows superior performance to SDEMf and SDMF in image restoration.

Table 1 lists the PSNR of the proposed algorithm, SDMF, SDEMf, and wavelet thresholding for images corrupted with Gaussian noise of zero mean and different standard deviations. It is obvious from Table 1 that our proposed method with Daubechies filters shows superior restoration performance over SDMF, SDEMf, and wavelet thresholding.

Also, we investigated the effect of the wavelet decomposition level on our method and noted that the restoration process became worse with deeper decomposition. Figure 9(a) plots 2-level decomposition of the noisy image using the lifting-based DB4 filter at PSNR=24.63. Figure 9(b) depicts the restored image of Fig. 9(a) at PSNR=33.13 by the proposed method. Figure 9(c) illustrates the 3-level

decomposition of the noisy image using the lifting-based DB4 filter at PSNR=24.63. Figure 9(d) shows the restored image of Fig. 9(c) at PSNR=30.12 by the proposed method.

Figure 10 shows a comparison of our proposed method with wavelet hard and soft thresholding.

VI. Conclusion

We have proposed an image restoration method of using a lifting-based wavelet domain e-median filter, which exhibits improved performance for additive white Gaussian noise removal. The effects of increasing the number of decomposition levels and the different kinds of wavelet filters on the proposed method have been investigated. Our experiments indicate that the image restoration performance related to the wavelet decomposition level becomes worse with deeper decomposition. Only the Daubechies wavelet can get the exact wave times in the expectative high frequency to express an object's profile. In other words, the Daubechies

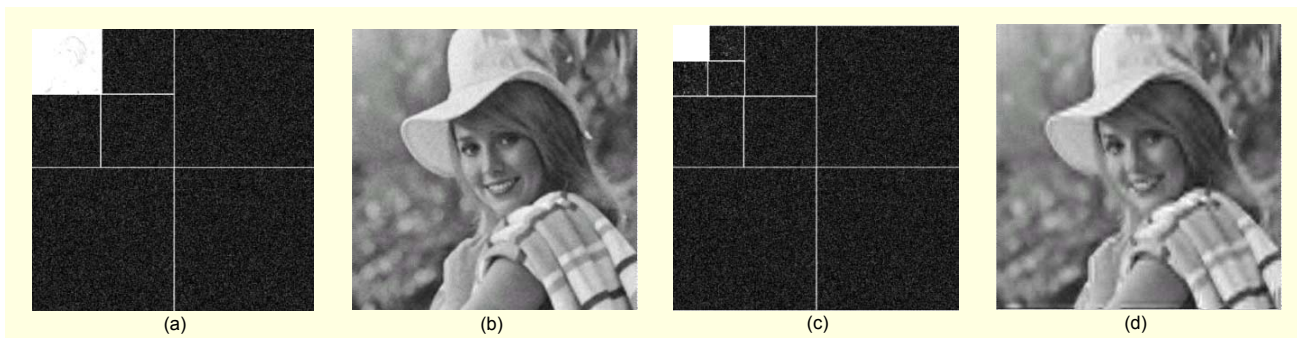


Fig. 9. (a) 2-level decomposition of noisy 512×512 Elaine image (PSNR=24.63), (b) restored image of Fig. 8(a) by proposed method with DB4 filter (PSNR=33.13), (c) 3-level decomposition of noisy 512×512 Elaine image (PSNR=24.63), and (d) restored image of Fig. 8(c) by proposed method with DB4 filter (PSNR=30.12).

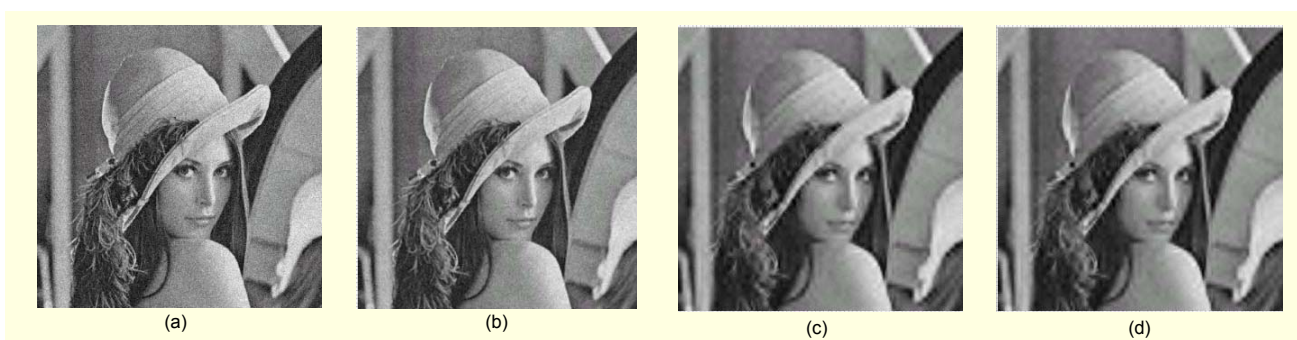


Fig. 10. (a) Corrupted image (PSNR=22.13), (b) the result of the proposed method with DB4 (PSNR=29.52), (c) the result of wavelet thresholding (universal hard thresholding at PSNR=28.09), and (d) the result of wavelet thresholding (universal soft thresholding at PSNR=26.93).

wavelet function has stronger ability to separate noises than other wavelets. The proposed method showed better performance using the DB4 wavelet filter. When the PSNR is low, transforming an image to the lifting-based wavelet domain produces better results than directly applying an e-median filter in the spatial domain. LBWDEMF alleviates the problem of encountering root sub-images at an early stage of iterations and makes further improvement possible. In other words, each of the sub-bands is processed independently in the wavelet domain by an e-median filter. In contrast, SDEMF degrades image quality after a few iterations due to encountering the root image at an early stage. It has been seen from the experimental results and visual observation of restored images that the proposed algorithm outperforms the other methods under study. The better performance of the proposed technique is due to a combined effect of the e-median filter and wavelet transform.

References

- [1] D.L. Donoho, "Denoising by Soft Thresholding," *IEEE Trans. Inform. Theory*, vol. 41 no. 3, 1995, pp. 613-627.
- [2] D.L. Donoho and I.M. Johnstone, "Ideal Spatial Adaptation via Wavelet Shrinkage," *Biometrika*, vol. 81, no. 3, 1994, pp. 425-455.
- [3] D.L. Donoho and I.M. Johnstone, "Adapting to Unknown Smoothness via Wavelet Shrinkage," *J. of the American Statistical Assoc.*, vol. 90, no. 432, 1995, pp. 1200-1224.
- [4] F. Abramovich, T. Sapatinas, and B.W. Silverman, "Wavelet Thresholding via a Bayesian Approach," *J. R. Statist. Soc., ser. B*, vol. 60, 1998, pp. 725-749.
- [5] A. Chambolle, R.A. DeVore, N. Lee, and B.J. Lucier, "Nonlinear Wavelet Image Processing: Variational Problems, Compression, and Noise Removal through Wavelet Shrinkage," *IEEE Trans. Image Processing*, vol. 7, 1998, pp. 319-335.
- [6] Ergun Erçelebi, "Electrocardiogram Signals De-Noising Using Lifting-Based Discrete Wavelet Transform," *Computers in Biology and Medicine*, vol. 34, Issue 6, Sept. 2004, pp. 479-493.
- [7] L.I. Rudin, S. Osher, and E. Fatemi, "Nonlinear Total Variation Based Noise Removal Algorithms," *Physica D*, vol. 60, 1992, pp. 259-268.
- [8] J. Astola and P. Kousmane, *Fundamentals of Nonlinear Digital Filtering*, CRC Press, 1997.
- [9] Pitas and A.N. Venetsanopoulos, *Nonlinear Digital Filters*, Kluwer Academic Press, 1990.

- [10] B.I. Justusson, *Median Filtering: Statistical Properties, Two-Dimensional Digital Signal Processing II*, ed. by T.S.Huang, Springer Verlag, NY, 1981.
- [11] A.K. Jain, *Fundamentals of Digital Image Processing*, Prentice Hall, NJ, 1989.
- [12] S.K. Mitra and G.L. Sicuranza, *Nonlinear Image Processing*, Academic Press, 2001.
- [13] M. Haseyama, M. Takezawa, K. Kondo, and H. Kitajima, "An Image Restoration Method Using IFS," *ICIP 2000*, Vancouver, Canada, Sept. 2000.
- [14] S.M. Mahbubur Rahman and Md. Kamrul Hasan, *Wavelet-Domain Iterative Center Weighted Median Filter for Image Denoising*, vol. 93, no. 5, 2003, pp. 1001-1012.
- [15] W. Sweldens, "The Lifting Scheme: A New Philosophy in Biorthogonal Wavelet Constructions," *Wavelet Applicat. Signal Image Process.*, vol. 2569, 1995, pp. 68-79.
- [16] W. Sweldens, "The Lifting Scheme: a Custom-Design Construction of Biorthogonal Wavelets," *Appl. Comput. Harmon. Anal.*, vol. 3, no. 2, 1996, pp. 186-200.
- [17] W. Sweldens, "The Lifting Scheme: a Construction of Second-Generation Wavelets," *SIAM J. Math. Anal.*, vol. 29, no. 2, 1997, pp. 511-546.
- [18] I. Daubechies and W. Sweldens, "Factoring Wavelet Transforms into Lifting Steps," *J. Fourier Anal. Appl.*, vol. 4, no. 3, 1998, pp. 247-269.
- [19] E. Ergun, "Second-Generation Wavelet Transform-Based Pitch Period Estimation and Voiced/Unvoiced Decision for Speech Signals," *Int. J. of Applied Acoustics*, vol. 64, no. 1, 2003, pp. 25-41.
- [20] S.G. Mallat, "Multiresolution Approximation and Wavelet Orthogonal Bases of $L^2(R)$," *Trans. Amer. Math. Soc.*, vol. 315, no. 1, 1989, pp. 69-87.
- [21] I. Daubechies, *Ten Lectures on Wavelets*, CBMS-NSF Regional Conf. Series in Applied Mathematics, vol. 61, SIAM, PA, 1992.



Sema Koç graduated from Gaziantep University in 1996. She earned the MSc degree from Gaziantep University in 1999, and the PhD degree from Gaziantep University in 2005, all in electrical and electronics engineering. Currently, she is a Research Assistant in the Electrical and Electronic Engineering Department at the University of Gaziantep Turkey, and is working on volume graphics and image processing.



Ergun Ercelebi received the BSEE degree from the Middle East Technical University (M.E.T.U.) in 1990, the MSEE degree from University of Gaziantep in 1992, and the PhD degree in electrical and electronics engineering from University of Gaziantep in 1999. From 1990 to 1999 he was a Research Assistant at the University of Gaziantep. Since 2000, he has been acting Assistant Professor of electrical and electronics engineering at University of Gaziantep. His research interest includes wavelet analysis, digital watermarking, speech enhancement, biomedical signal processing, speech recognition, image coding, and adaptive digital filters.